# THE EFFECTS OF NOISE AND BANDLIMITING ON A ONE DIMENSIONAL TIME DEPENDENT INVERSE SCATTERING TECHNIQUE

J. P. Corones and R. J. Krueger
Ames Laboratory, USDOE, Iowa State University
Ames, IA 50011

C. R. Vogel
Iowa State University, Ames, IA 50011

## INTRODUCTION

In realistic settings data used as input to any inverse scattering algorithm is bandlimited and corrupted by noise. At present there is no satisfactory way to determine the extent to which reconstructions using imperfect data are degraded due to noise and bandlimiting. In this paper, this problem is considered from the point of view of the sensitivity matrix of the mapping that transforms, via an inverse scattering algorithm outlined below,[1] reflection data to information about material profiles of media.

## TIME DOMAIN INVERSION AND SOURCES OF ERROR

The entire discussion is pertinent to the wave equation

$$u_{xx} - u_{tt} + A(x)\, u_x = 0 \qquad (1)$$

This equation with various choices of A(x) models electromagnetic, transverse elastic or longitudinal elastic waves propagating in a stratified medium. The independent variable x is a travel time coordinate.[1]

Consider a slab of inhomogeneous material with left edge at x=0 and right edge at x=1 and suppose that the medium is homogeneous for x<0, x>1. If a field $u^+(t)$ with ($u^+(t)$=0 for t<0) is incident upon the slab from the left a reflected field $u^-(t)$ propagating to the left results. It is known[1] that

$$u^-(t) = \int_0^t R(0,t-s)u^+(s)ds. \qquad (2)$$

The function R(0,t) is the reflection kernel for the slab. It can be shown that R(0,t) is the boundary value for a function R(x,t) which satisfies

$$R_x(x,t) - 2R_t(x,t) + \frac{A(x)}{2} \int_0^t R(x,s)R(x,t-s)ds=0, \quad 0<x<1 \qquad (3)$$

$$R(x,0^+) = -\frac{A(x)}{4}, \quad 0 < x < 1$$

$$R(1,t) = 0, \quad t > 0$$

This system of equations and initial/boundary conditions are the basis for an inverse scattering algorithm explicitly discussed in (1).

This algorithm starts with R(0,t), the reflection kernel or impulse response of the slab, and yields A(x), the material profile of the medium. Thus it provides a mapping

$$F: \ R(0,t) \rightarrow A(x) \qquad (4)$$

$$F(R(0,t)) = A(x)$$

Examples of the numerical implementation of the algorithm are shown in figures 1, 9 and 17. In each case, the reconstruction of the profile A(x) is indistinguishable from the true profile. The broken line in each figure is the reconstruction of the profile using the linearized approximation to equation (3), i.e., the convolution term is neglected. The linearized approximation is a single scattering approximation, here called the Bremmer approximation (Born like), and yields a good reconstruction of the weak scatterer in Fig. 1. Naturally, the approximation degrades as the strength of the scatterer increases, compare Figure 9 and Figure 17.

In practice, R(0,t) must be recovered from an expression of the form

$$T_1 * u^-(t) = \int_0^t R(0,t-s)u^+(s)ds + \eta(t)$$

where $T_1$ is the transfer function of the measuring instrument and $\eta(t)$ models the noise in the system. Thus in practice the starting point of the algorithm is an estimate of R(0,t) which will be denoted by $\bar{R}(0,t)$. How the fact that one starts with an approximated R ($\bar{R}$) influences the computed values of A(x) is the subject of this report.

## SENSITIVITY ANALYSIS VIA THE SVD OF THE JACOBIAN

The solution of problem (3) defines an operator F given in (4) taking the reflection kernel R(0,t), $t \geq 0$, to the function A(x), $x \geq 0$. This operator F is differentiable, so that

$$\Delta A = F(R) - F(\bar{R}) \approx F'(\bar{R})\Delta R. \qquad (5)$$

Here $\bar{R}$ is an estimate of the true R and $\Delta R$ is a perturbation of R which represents error in estimating R due to, say, bandlimiting or instrument noise. The linear operator F'(R), which is the Jacobian of

F, determines the effect on the reconstruction of A(x) of the perturbation $\Delta R$. We will present a quantitative description of this effect in terms of the singular value decomposition (SVD) of F'(R).

## COMPUTATION OF THE JACOBIAN

Given discrete data $R_j = R(0,t_j)$, $j=1,\ldots,n$, we compute the discrete approximation $A_i$ to $A(x_i)$, $i=1,\ldots,n$, as outlined in (1). The discrete approximation to the Jacobian F'(R) is simply the matrix $\bar{F}'(R)$ with entries

$$[\bar{F}'(R)]_{ij} = \frac{\partial A_i}{\partial R_j} \quad , \; 1 \leq i, j \leq n \tag{6}$$

which are estimated numerically by means of the finite difference approximation

$$\frac{A_i(R+he_j) - A_i(R-he_j)}{2h} \tag{7}$$

where h is the step size and $e_j$ is the vector whose $j^{th}$ entry is 1 and whose remaining entries are all 0.

## THE SVD ANALYSIS

It can be shown (2) that the Jacobian has the form

$$F'(R) = -4I + K \tag{8}$$

where I is the identity and K is an integral operator. The discrete approximation also shares this form, i.e.,

$$\bar{F}'(R) = -4I + \bar{K} \tag{9}$$

where now I is the nxn identity matrix and $\bar{K}$ is an nxn matrix corresponding to K. Since K is an integral operator, we expect that the singular values of K decay to zero. A similar singular value structure is observed for the matrix $\bar{K}$ (see Figs. 8, 16, 24).

Let $s_j$, $j=1,\ldots,n$ denote the singular values of $\bar{K}$ (in decreasing order of magnitude) and let $u_j$ and $v_j$ denote, respectively, the corresponding left and right singular vectors of $\bar{K}$. The singular value decomposition of $\bar{K}$ is the matrix decomposition $\bar{K}=USV^T$ where S is the nxn diagonal matrix with $j^{th}$ diagonal entry $s_j$, U contains the left singular vectors $u_j$ as its columns, and V contains the right singular vectors $v_j$ as its columns. In addition, U and V are orthogonal matrices, i.e., $U^TU = UU^T = I = V^TV = VV^T$. We can write the perturbation in R as $\Delta R = \sum_{j=1}^{n} r_j v_j$. Similarly, the corresponding perturbation in A may be written $\Delta A = \sum_{j=1}^{n} a_j u_j$. Then in terms of the singular components, equation (5) becomes

$$\Delta A = \sum_{j=1}^{n} a_j \mu_j \approx \sum_{j=1}^{n} r_j (-4I+\bar{K})v_j$$

$$= -4\Delta R + \sum_{j=1}^{n} (r_j s_j) u_j \qquad (10)$$

If $\bar{K}$ were the zero matrix, then all the singular values $s_j$ would be zero and the effect of a small perturbation $\Delta R$ would be approximately a perturbation of $-4\Delta R$ in A. In the (weak scattering) Bremmer approximation, $\Delta R$ gives exactly a perturbation $\Delta A = -4\Delta R$ in A. As the strength of the scatterer increases, the size of the matrix $\bar{K}$, as measured by the magnitudes of the singular values $s_j$, also increases (compare Fig. 8 with Figs. 16 and 24).

Effects of the perturbation $\Delta R$ on the reconstruction of A(x) vary with the modes of the perturbation. For instance, the loss of high frequency information has little effect on the reconstruction in either the weak (Fig. 4) or the strong (Figs. 12, 20) scattering cases. (In these figures, only the ten lowest frequency components of R have been retained.) This can be explained in terms of the SVD as follows: Singular vectors $v_j$ corresponding to small singular values $s_j$ are highly oscillatory (see Figs. 7, 15, 23 for plots of the 100$^{th}$ singular vectors). Thus, high frequency information is concentrated in the coefficients $r_j$ in the expansion $\Delta R = \sum_{j=1}^{n} r_j v_j$ for which the corresponding $s_j$'s are nearly zero. Consequently, we see from equation (10) that the effect of a high frequency perturbation $\Delta R$ is approximately a perturbation $\Delta A = -4\Delta R$ in the reconstruction of A(x).

On the other hand, a low frequency perturbation $\Delta R$ such as that resulting from the loss of low frequency information causes a significant degradation in the reconstruction of A(x). Singular vectors corresponding to the larger singular values are slowly varying (see Figs. 5, 13, and 21), and have large low frequency components. Thus, low frequency information is concentrated in the coefficients $r_j$ for which the corresponding $s_j$'s are large, and equation (10) suggests a large perturbation in A(x). This effect can be seen in Figs. 2, 3, 10, 11, 18, and 19. The first figure in each pair (2, 10, 18) shows a reconstruction with DC content of R missing, while the second figure in each pair (3, 11, 19) shows reconstructions with the DC and next highest frequency in R missing. Figures 6, 14 and 22 show the 20$^{th}$ singular vector for each profile.

In Fig. 25, white noise is added to the reflection kernel R for the medium displayed in Fig. 9 and the reconstructed A appears in Fig. 26. To generate Fig. 27, the noisy kernel R was first smoothed before the inversion. Even though the signal to noise ratio of 2.1 is large, little large scale degradation in A(x) occurs in either case. The degradation which does appear is due primarily to low frequency components in the noise.

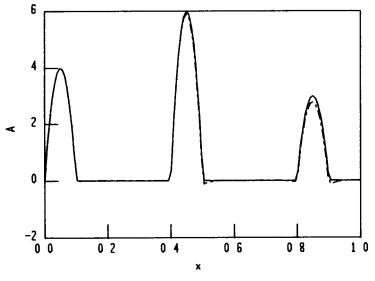


Fig. 1

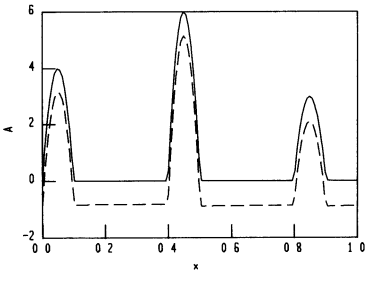


Fig. 2

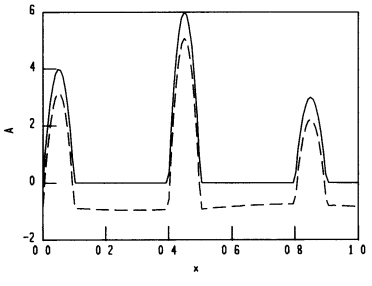


Fig. 3

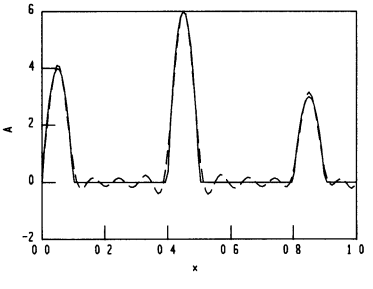


Fig. 4

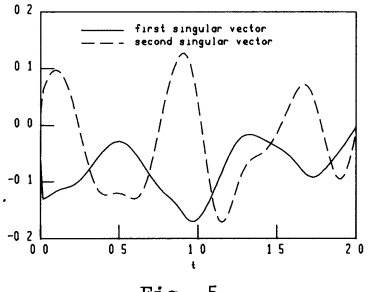


Fig. 5

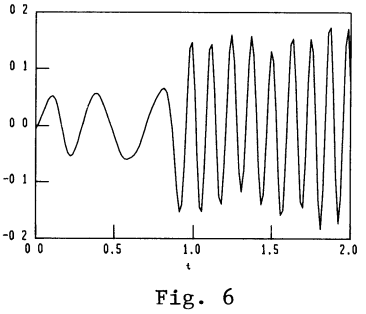


Fig. 6

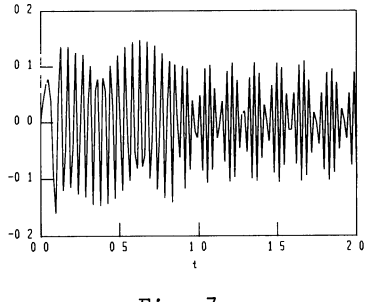


Fig. 7

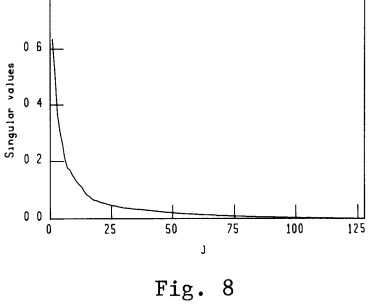


Fig. 8

Figures 1-8 refer to the medium shown by the solid line in Fig. 1.

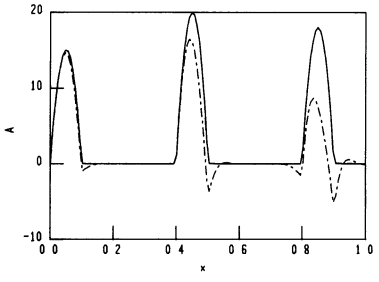


Fig. 9

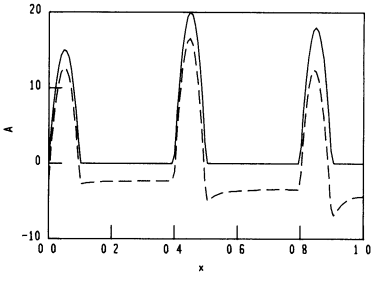


Fig. 10

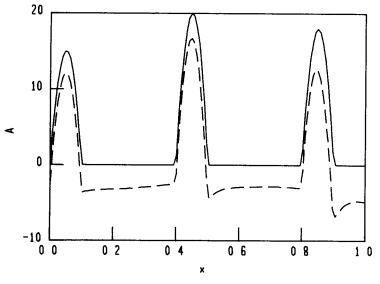


Fig. 11

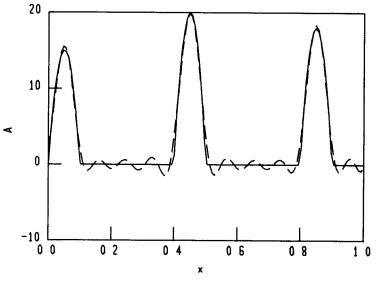


Fig. 12

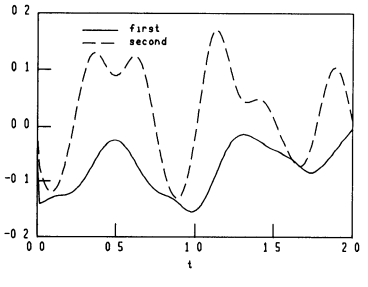


Fig. 13

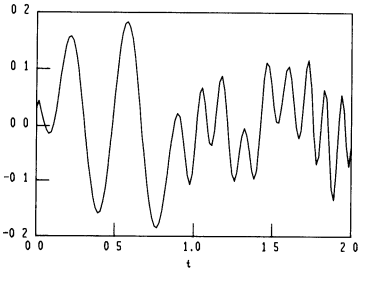


Fig. 14

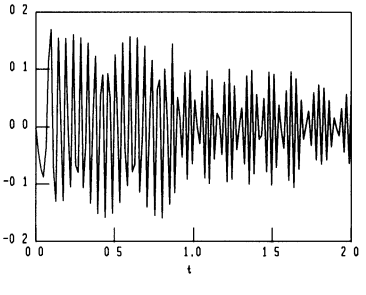


Fig. 15

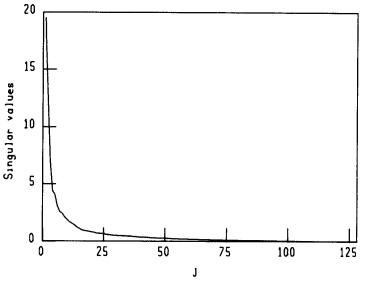


Fig. 16

Figures 9-16 refer to the medium shown by the solid line in Fig. 9.

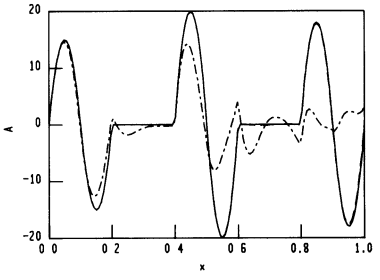


Fig. 17

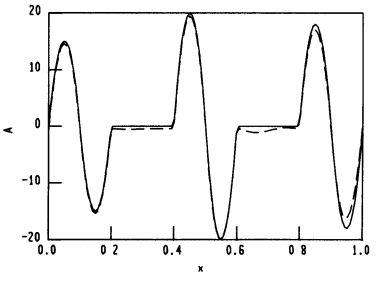


Fig. 18

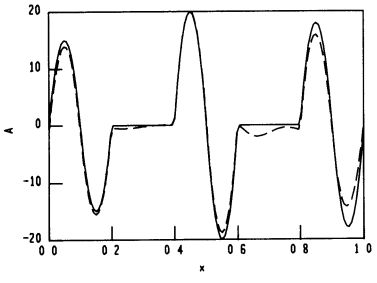


Fig. 19

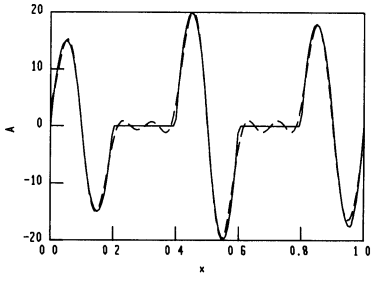


Fig. 20

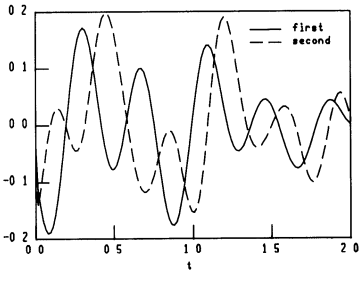


Fig. 21

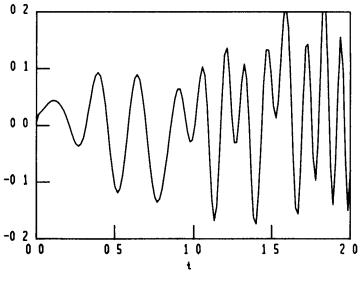


Fig. 22

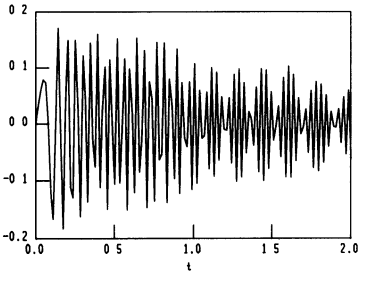


Fig. 23

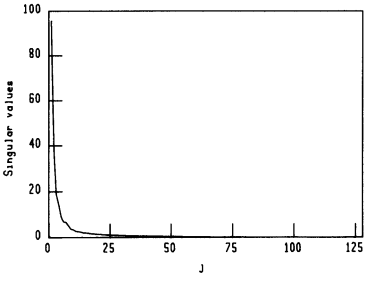


Fig. 24

Figures 17-24 refer to the medium shown by the solid line in Fig. 17.

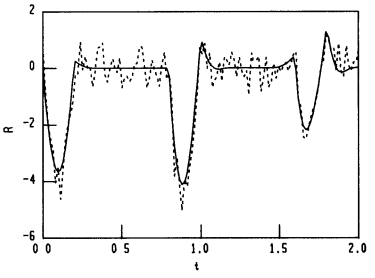


Fig. 25
Reflection kernel (solid line) and kernel with additive white noise (broken line).

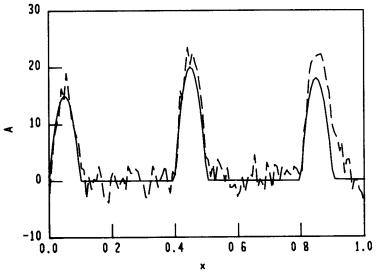


Fig. 26
Reconstruction using noisy data.

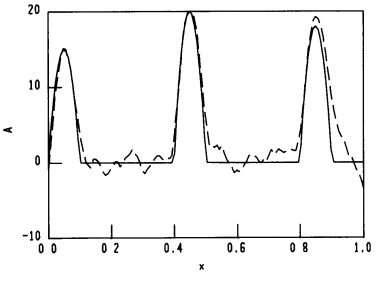


Fig. 27
Reconstruction with smoothed noisy data.

ACKNOWLEDGEMENT

This work was supported by the United States Department of Energy, Contract No. W-7405-eng-82, Division of Engineering, Mathematics and Geosciences, budget code KC-04-01-03, and by the Office of Naval Research, Contract N0014-83-K-0038.

REFERENCES

1. J. P. Corones, M. E. Davison and R. J. Krueger, Direct and inverse scattering in the time domain via invariant imbedding equations, Acoust. Soc. Am. 74:1535 (1983).
2. C. R. Vogel, "A Banach space ODE framework for inverse scattering via invariant imbedding," preprint.